

# Identification of additional jets in the $t\bar{t}b\bar{b}$ events using a deep neural network

Jieun Choi, Tae Jeong Kim,<sup>\*</sup> Jongwon Lim, Jiwon Park, Yeonsu Ryou, and Juhee Song

*Department of Physics, Hanyang University, Seoul*

(Received 31 October 2019)

## Abstract

After the discovery of the Higgs boson, its consistency with the standard model has been tested extensively in many different channels. Importantly the coupling of the Higgs boson with the top quark was observed in the top quark pair production in association with the Higgs boson ( $t\bar{t}H$ ) in 2018. In the standard model, the Higgs boson decays to  $b\bar{b}$  with the largest branching fraction. To improve the sensitivity of the  $t\bar{t}H(b\bar{b})$  process, it is essential to understand the  $t\bar{t}b\bar{b}$  process precisely. In this paper, the two additional  $b$  jets in the  $t\bar{t}b\bar{b}$  process are identified in the lepton+jets channel by using minimum  $\Delta R(b, \bar{b})$  method or neural network with multiple variables. The performances of these two approaches are compared quantitatively. This study will provide valuable information towards precise measurement of differential cross sections as a function of properties of the additional  $b$  jets in the  $t\bar{t}b\bar{b}$  events.

PACS numbers: 14.65.Ha, 07.05.Mh

Keywords: Higgs, top quark, deep neural network

---

<sup>\*</sup>Electronic address: taekim@hanyang.ac.kr

## I. INTRODUCTION

After the discovery of the Higgs boson, its consistency with the standard model has been tested extensively in many different channels. Importantly the coupling of the Higgs boson with the top quark was observed in the top quark pair production in association with the Higgs boson ( $t\bar{t}H$ ) in 2018 [1, 2] directly. The branching fraction of the Higgs boson to  $b\bar{b}$  is the largest. Therefore,  $t\bar{t}H(b\bar{b})$  process can be measured with the best statistical precision. To improve the sensitivity of the  $t\bar{t}H(b\bar{b})$  process, it is essential to understand the  $t\bar{t}b\bar{b}$  process, precisely. The uncertainty on the theoretical NLO calculation is also large [3]. The inclusive cross sections of the  $t\bar{t}b\bar{b}$  process have been measured in the dilepton channel at  $\sqrt{s} = 13$  TeV by the CMS experiment [4]. The cross section in the hadronic channel is measured recently [5]. The inclusive and differential  $t\bar{t}b\bar{b}$  cross sections are also measured by the ATLAS experiment [6]. However, in the ATLAS measurement, the origin of the  $b$  jet is not identified. When it comes to measuring the differential cross section as a function of properties of the additional  $b$  jets, the origin of the  $b$  jet needs to be identified. In real data, it is very challenging since there is no single variable that can distinguish between additional  $b$  jets and the  $b$  jets from top quark decays. In the CMS experiment, using early data at  $\sqrt{s} = 8$  TeV, identifying the additional  $b$  jets was already attempted for the first time with a boosted decision tree in the dilepton channel [7]. In this Ref. [7], the differential cross sections as a function of the  $p_T$  and  $|\eta|$  of the the leading and subleading additional  $b$  jets, and  $\Delta R(b, \bar{b})$  and invariant mass  $m(b, \bar{b})$  of two additional  $b$  jets are measured. Recently, a deep neural network has been proposed to reconstruct the  $t\bar{t}$  events and compared with kinematic fitting [8]. In this paper, the two additional  $b$  jets in the  $t\bar{t}b\bar{b}$  process in the lepton+jets channel are identified using the minimum  $\Delta R(b, \bar{b})$  method or deep learning techniques. The performances of these two approaches are compared quantitatively. This study will provide valuable information towards precise differential cross section measurement in the lepton+jets channel. This measurement suffers from large combinatorial backgrounds. For example, if there are 6 jets in the clean  $t\bar{t}b\bar{b}$  events, the probability of identifying additional  $b$  jets with random choice is only around 7% ( $2/6 \times 1/5$ ) when we for sure there are two additional jets in the selected events. For this reason, the dilepton channel would have advantage compared to the lepton+jets channel. However, in the differential cross section measurements of  $t\bar{t}b\bar{b}$ , it is crucial to have larger statistics. Therefore, this study makes

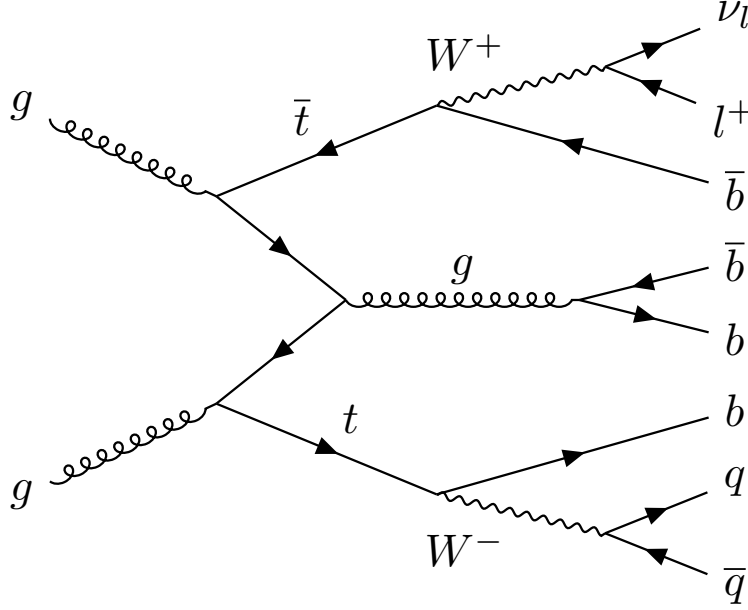


FIG. 1: A feynman diagram for the  $t\bar{t}b\bar{b}$  process in the lepton+jets where one of the W bosons decays hadronically.

use of the lepton+jet events which have larger cross section. The feynman diagram of  $t\bar{t}b\bar{b}$  process in the lepton+jets mode is shown in Fig. 1. This study focuses on finding the best combination of two additional b jets in the lepton+jets channel with different event selections for quantitative comparisons.

## II. SAMPLES

The simulated  $t\bar{t}b\bar{b}$  events in pp collisions are produced at a center-of-mass energy of 13 TeV. 10M events for the  $t\bar{t}b\bar{b}$  samples are generated by using the MADGRAPH5\_aMC@NLO program (v2.6.6) [9] at the leading order and are further interfaced to PYTHIA (v8.240) [10] for the hadronization. A W boson decays through MADSPIN [11]. The events are generated in a 4-flavor scheme, where the b quark has mass.

The generated events are processed by the detector simulation using DELPHES package (v3.4.1) [12] for the CMS detector. The physics objects used in this analysis are recon-

structured based on the particle-flow algorithm implemented in the DELPHES framework. In the DELPHES fast simulation, the final momenta of all the physics objects, such as electrons, muons and jets, are smeared as a function of transverse momentum  $p_T$  and pseudo-rapidity  $\eta$  so that they can represent the detector effects. The identification efficiencies of the electrons, muons and jets are also parameterized as functions of  $p_T$  and  $\eta$  based on information from the measurements using the CMS data [12]. The muon identification efficiency is set to 95% for the muons with momenta  $p_T > 10$  GeV and  $p_T < 100$  GeV. The electron identification efficiency is set to 95% for  $|\eta| > 1.5$  and 85% for  $1.5 < |\eta| < 2.5$ . The isolated muons and electrons are selected by applying a relative isolation of  $I_{rel} < 0.25$  and 0.12, respectively, where  $I_{rel}$  is defined as the sum of the surrounding energy from the particle-flow tracks, photons and neutral hadrons divided by the transverse momentum of the muon or electron. The particle-flow jets used in this analysis are clustered by using the particle-flow tracks and particle-flow towers. If the jet is already reconstructed as an isolated electron, muon or photon, the jet is excluded from further consideration. The b-tagging efficiency parameterized as a function of  $p_T$  and  $\eta$  of the jet following polynomial functions is around 50% at the tight-working point of the deep combined secondary vertex (DeepCSV) algorithm in the CMS measurement [13]. The corresponding fake b-tagging rates from the c-flavor and light flavor jet are set to around 2.6% and 0.1%, respectively.

Once events are produced, the  $t\bar{t}b\bar{b}$  process is defined based on the particle-level jets which are obtained by clustering all final-state particles at the generator level. A jet is considered as the additional b jet if the jet is matched to the last b quark not from a top quark within  $\Delta R(j, q) = \sqrt{\Delta\eta(j, q)^2 + \Delta\phi(j, q)^2} < 0.5$ , where j denotes jets at the generator level and q denotes the last b quark. The additional b jets are required to be within the experimentally accessible kinematic region of  $\eta < 2.5$  and  $p_T > 20$  GeV. At least two additional b jets should exist to be  $t\bar{t}b\bar{b}$  events.

### III. EVENT SELECTION

In the lepton+jets channel, at the reconstruction level, the event must have exclusively one lepton with  $p_T > 30$  GeV and  $\eta < 2.4$  at the preselection (**S1**). Jets are selected with the threshold of  $p_T > 30$  GeV and  $\eta < 2.5$ . The  $t\bar{t}b\bar{b}$  event has the final state of four b jets and two jets from one of two W bosons in top quark decays. However, the efficiencies of

the jet reconstruction and b jet tagging algorithms are not 100%. Some of the  $t\bar{t}b\bar{b}$  events have less number of jets at the reconstruction level. Therefore, starting from at least 2 jet requirement, the events are split into 12 datasets based on the number of the jets (**S2**) and b-tagged jets (**S3**) inclusively. The number of selected events and corresponding acceptance for each event selection are shown in Table I. These number of events are used for the  $\Delta R$  and deep neural network methods in following sections.

$N_j$	$N_b$	$t\bar{t}b\bar{b}$ events	S1 ( $N_l = 1$ )	S2, S3 ( $\geq N_j, \geq N_b$ )	Acceptance (%)
2	2	1888043	561273	275117	2.75
3				273659	2.74
4				259712	2.60
5				213440	2.13
6				137136	1.37
3	3			91961	0.92
4				90187	0.90
5				79489	0.79
6				55439	0.55
4	4			15329	0.15
5				14638	0.15
6				11478	0.11

TABLE I: The number of events in each event selection based on the number of the jets and b-tagged jets inclusively and corresponding acceptances are shown.

#### IV. MINIMUM $\Delta R$ ANALYSIS

One simple approach to identify two additional b jets is to select two b-tagged jets with the minimum angle of  $\Delta R$  between them. This method is based on the fact that the additional b jets are from the gluon splitting to  $b\bar{b}$ . If the selected jet is matched to any of additional b jets at the generation level within  $\Delta R < 0.4$ , the jet is considered to be from additional b jet. Both of two selected jets should be matched to be a correct combination. Then, the matching efficiency is defined as the ratio of the number of “*matched*” events to the number of events after each event selection. The matching efficiency is used as a figure of merit to check the performance in this analysis. The  $\Delta R$  in the correct combination tends to have smaller angle between two jets so it can be distinguished from the wrong combinations, as shown in Section V.

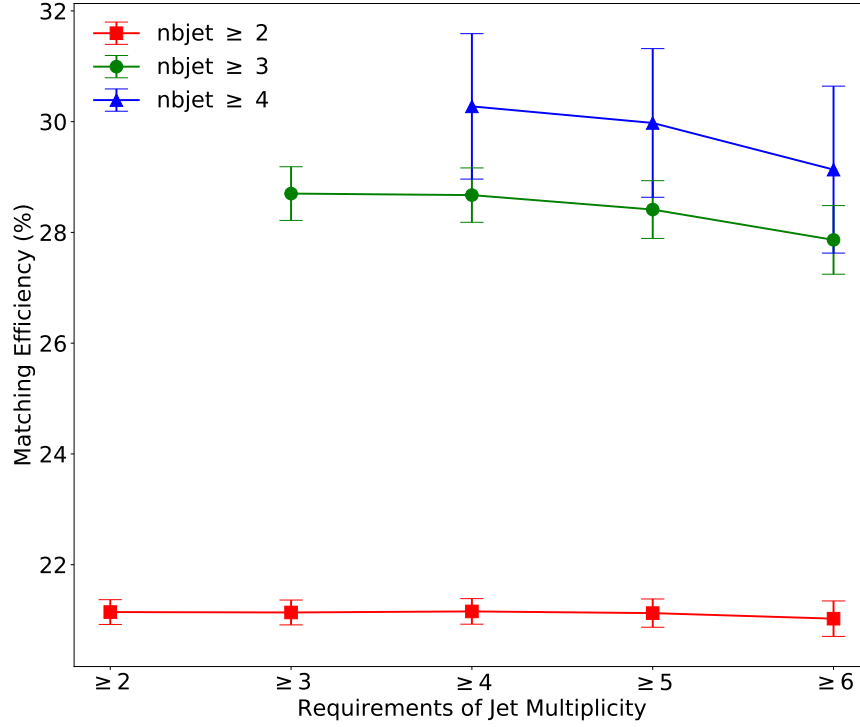


FIG. 2: Matching efficiency from the  $\Delta R$  analysis is shown as a function of number of jets. The results with different requirements of number of b-tagged jets are also shown with rectangle mark for at least 2 b-tagged jets, circle for 3 b-tagged jets and triangle for 4 b-tagged jets (color online).

After the preselection, events are selected by requiring at least 2 jets and at least 2 of which are b-tagged jets. With requirements on various (b) jet multiplicities, the performance is tested in each dataset as the matching efficiency can be different. With the  $\Delta R$  approach, the matching efficiency is calculated as around 21% with the requirement of at least 2 b-tagged jets, 28% for at least 3 b-tagged jets and 30% for at least 4 b-tagged jets. Figure 2 shows the matching efficiency as a function of number of jets and b-tagged jets with different colors. All of these cases, the matching efficiencies are worse slightly as more jets are required.

In this result, there are two aspects. Due to large combinatorial background with higher jet multiplicity, these additional wrong combinations could decrease the matching efficiency. On the contrary, if the number of b-tagged jets is larger, there would be more chance to have the correct assignment. Figure 3 shows the fraction of number of events which have the matchable combination with respect to the selected events. As expected, the ratio significantly goes up with the requirement of at least 3 b-tagged jets.

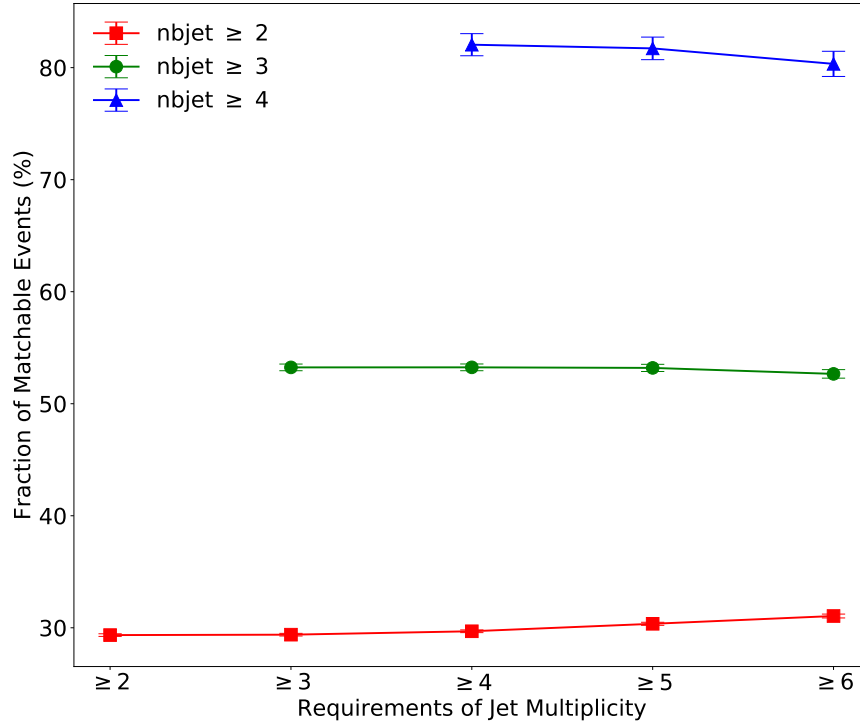


FIG. 3: Fraction of matchable events in the selected dataset as a function of number of jets. The results with different requirements of number of b-tagged jets are also shown with rectangle mark for 2 b-tagged jets, circle for 3 b-tagged jets and triangle for 4 b-tagged jets (color online).

## V. DEEP NEURAL NETWORK ANALYSIS

As the second approach, the deep neural network with multi-variables is used to increase the matching efficiency. The goal of the neural network is to make use of multi-variables from the properties of the selected objects to decide which combination is most probable to originate from gluon splitting. The variables are selected considering all possible combinations of four-vector of the final state objects such as selected two b-tagged jets, a lepton, a reconstructed hadronic W boson and missing transverse energy (MET). The list of total 78 variables are shown in Tables II and III.

We will use a deep neural network for the binary classification. For this classification, if two selected jets among the combinations of all b-tagged jets are matched to additional b jets, this combination is considered as “*signal*”. All other combinations are considered as “*background*”. For example, when there are three b-tagged jets, there are three possible combinations of two jets. Possibly one combination is signal and other two combinations

Variable	Description
$\Delta R(b, \bar{b})$	$\Delta R$ between two b-tagged jets
$\Delta \eta(b, \bar{b})$	$\Delta \eta$ between two b-tagged jets
$\Delta \phi(b, \bar{b})$	$\Delta \phi$ between two b-tagged jets
$p_T(b, \bar{b})$	$p_T$ of two b-tagged jets
$\eta(b, \bar{b})$	$\eta$ of two b-tagged jets
$m(b, \bar{b})$	Mass of two b-tagged jets
$m_T(b, \bar{b})$	Transverse mass of two b-tagged jets
$p_T(b, \bar{b})$	Scalar sum of $p_T$ of two b-tagged jets
$\Delta R(b\bar{b}, l)$	$\Delta R$ between two b-tagged jets and lepton
$\Delta \eta(b\bar{b}, l)$	$\Delta \eta$ between two b-tagged jets and lepton
$\Delta \phi(b\bar{b}, l)$	$\Delta \phi$ between two b-tagged jets and lepton
$p_T(b\bar{b}, l)$	$p_T$ of two b-tagged jets and lepton
$\eta(b\bar{b}, l)$	$\eta$ of two b-tagged jets and lepton
$m(b\bar{b}, l)$	Mass of two b-tagged jets and lepton
$m_T(b\bar{b}, l)$	Transverse mass of two b-tagged jets and lepton
$p_T(b\bar{b}, l)$	Scalar sum of $p_T$ of two b-tagged jets and lepton
$\Delta R(b\bar{b}, \nu)$	$\Delta R$ between two b-tagged jets and missing transverse energy (MET)
$\Delta \eta(b\bar{b}, \nu)$	$\Delta \eta$ between two b-tagged jets and MET
$\Delta \phi(b\bar{b}, \nu)$	$\Delta \phi$ between two b-tagged jets and MET
$p_T(b\bar{b}, \nu)$	$p_T$ of two b-tagged jets and MET
$\eta(b\bar{b}, \nu)$	$\eta$ of two b-tagged jets and MET
$m(b\bar{b}, \nu)$	Mass of two b-tagged jets and MET
$m_T(b\bar{b}, \nu)$	Transverse mass of two b-tagged jets and MET
$p_T(b\bar{b}, \nu)$	Scalar sum of $p_T$ of two b-tagged jets and MET
$\Delta R(b1, l)$	$\Delta R$ between b-tagged jet with the highest $p_T$ and lepton
$\Delta \eta(b1, l)$	$\Delta \eta$ between b-tagged jet with the highest $p_T$ and lepton
$\Delta \phi(b1, l)$	$\Delta \phi$ between b-tagged jet with the highest $p_T$ and lepton
$p_T(b1, l)$	$p_T$ of b-tagged jet with the highest $p_T$ and lepton
$\eta(b1, l)$	$\eta$ of b-tagged jet with the highest $p_T$ and lepton
$m(b1, l)$	Mass of b-tagged jet with the highest $p_T$ and lepton
$m_T(b1, l)$	Transverse mass of b-tagged jet with the highest $p_T$ and lepton
$p_T(b1, l)$	Scalar sum of $p_T$ of b-tagged jet with the highest $p_T$ and lepton
$\Delta R(b1, \nu)$	$\Delta R$ between b-tagged jet with the highest $p_T$ and MET
$\Delta \eta(b1, \nu)$	$\Delta \eta$ between b-tagged jet with the highest $p_T$ and MET
$\Delta \phi(b1, \nu)$	$\Delta \phi$ between b-tagged jet with the highest $p_T$ and MET
$p_T(b1, \nu)$	$p_T$ of b-tagged jet with the highest $p_T$ and MET
$\eta(b1, \nu)$	$\eta$ of b-tagged jet with the highest $p_T$ and MET
$m(b1, \nu)$	Mass of b-tagged jet with the highest $p_T$ and MET
$m_T(b1, \nu)$	Transverse mass of b-tagged jet with the highest $p_T$ and MET
$H_T(b1, \nu)$	Scalar sum of $p_T$ of b-tagged jet with the highest $p_T$ and MET

TABLE II: Input variables for deep neural network (Continued in Table III)

are backgrounds. Therefore, requiring more jets implies more background in training. The signal and background distributions of the most distinguished variables are shown in Fig. 4.

The dataset in each event selection is split into two datasets, 80% of data to train model and remaining 20% for test. Hyper-parameters of the neural network such as number of



Variable	Description
$\Delta R(b1, W)$	$\Delta R$ between b-tagged jet with the highest $p_T$ and W
$\Delta \eta(b1, W)$	$\Delta \eta$ between b-tagged jet with the highest $p_T$ and W
$\Delta \phi(b1, W)$	$\Delta \phi$ between b-tagged jet with the highest $p_T$ and W
$p_T(b1, W)$	$p_T$ of b-tagged jet with the highest $p_T$ and W
$\eta(b1, W)$	$\eta$ of b-tagged jet with the highest $p_T$ and W
$m(b1, W)$	Mass of b-tagged jet with the highest $p_T$ and W
$m_T(b1, W)$	Transverse mass of b-tagged jet with the highest $p_T$ and W
$p_T(b1, W)$	Scalar sum of $p_T$ of b-tagged jet with the highest $p_T$ and W
$\Delta R(b2, l)$	$\Delta R$ between b-tagged jet with the second highest $p_T$ and lepton
$\Delta \eta(b2, l)$	$\Delta \eta$ between b-tagged jet with the second highest $p_T$ and lepton
$\Delta \phi(b2, l)$	$\Delta \phi$ between b-tagged jet with the second highest $p_T$ and lepton
$p_T(b2, l)$	$p_T$ of b-tagged jet with the second highest $p_T$ and lepton
$\eta(b2, l)$	$\eta$ of b-tagged jet with the second highest $p_T$ and lepton
$m(b2, l)$	Mass of b-tagged jet with the second highest $p_T$ and lepton
$m_T(b2, l)$	Transverse mass of b-tagged jet with the second highest $p_T$ and lepton
$p_T(b2, l)$	Scalar sum of $p_T$ of b-tagged jet with the second highest $p_T$ and lepton
$\Delta R(b2, \nu)$	$\Delta R$ between b-tagged jet with the second highest $p_T$ and MET
$\Delta \eta(b2, \nu)$	$\Delta \eta$ between b-tagged jet with the second highest $p_T$ and MET
$\Delta \phi(b2, \nu)$	$\Delta \phi$ between b-tagged jet with the second highest $p_T$ and MET
$p_T(b2, \nu)$	$p_T$ of b-tagged jet with the second highest $p_T$ and MET
$\eta(b2, \nu)$	$\eta$ of b-tagged jet with the second highest $p_T$ and MET
$m(b2, \nu)$	Mass of b-tagged jet with the second highest $p_T$ and MET
$m_T(b2, \nu)$	Transverse mass of b-tagged jet with the second highest $p_T$ and MET
$p_T(b2, \nu)$	Scalar sum of $p_T$ of b-tagged jet with the second highest $p_T$ and MET
$\Delta R(b2, W)$	$\Delta R$ between b-tagged jet with the second highest $p_T$ and W
$\Delta \eta(b2, W)$	$\Delta \eta$ between b-tagged jet with the second highest $p_T$ and W
$\Delta \phi(b2, W)$	$\Delta \phi$ between b-tagged jet with the second highest $p_T$ and W
$p_T(b2, W)$	$p_T$ of b-tagged jet with the second highest $p_T$ and W
$\eta(b2, W)$	$\eta$ of b-tagged jet with the second highest $p_T$ and W
$m(b2, W)$	Mass of b-tagged jet with the second highest $p_T$ and W
$m_T(b2, W)$	Transverse mass of b-tagged jet with the second highest $p_T$ and W
$p_T(b2, W)$	Scalar sum of $p_T$ of b-tagged jet with the second highest $p_T$ and W
$p_T(b1)$	$p_T$ of b-tagged jet with the highest $p_T$
$\eta(b1)$	$\eta$ of b-tagged jet with the highest $p_T$
$e(b1)$	energy of b-tagged jet with the highest $p_T$
$p_T(b2)$	$p_T$ of b-tagged jet with the second highest $p_T$
$\eta(b2)$	$\eta$ of b-tagged jet with the second highest $p_T$
$e(b2)$	energy of b-tagged jet with the second highest $p_T$

TABLE III: Continued from Table II

epochs, number of layers and number of nodes per each hidden layer are optimized based on the matching efficiency calculated on the test dataset. To minimize overtraining, regularization technique of L2 regularization, batch normalization [14] and dropout [15] dropping out nodes by 8% in each hidden layer are used. Two main hyperparameters of the number of layers and the number of nodes in each hidden layer are configured by scanning the 2D

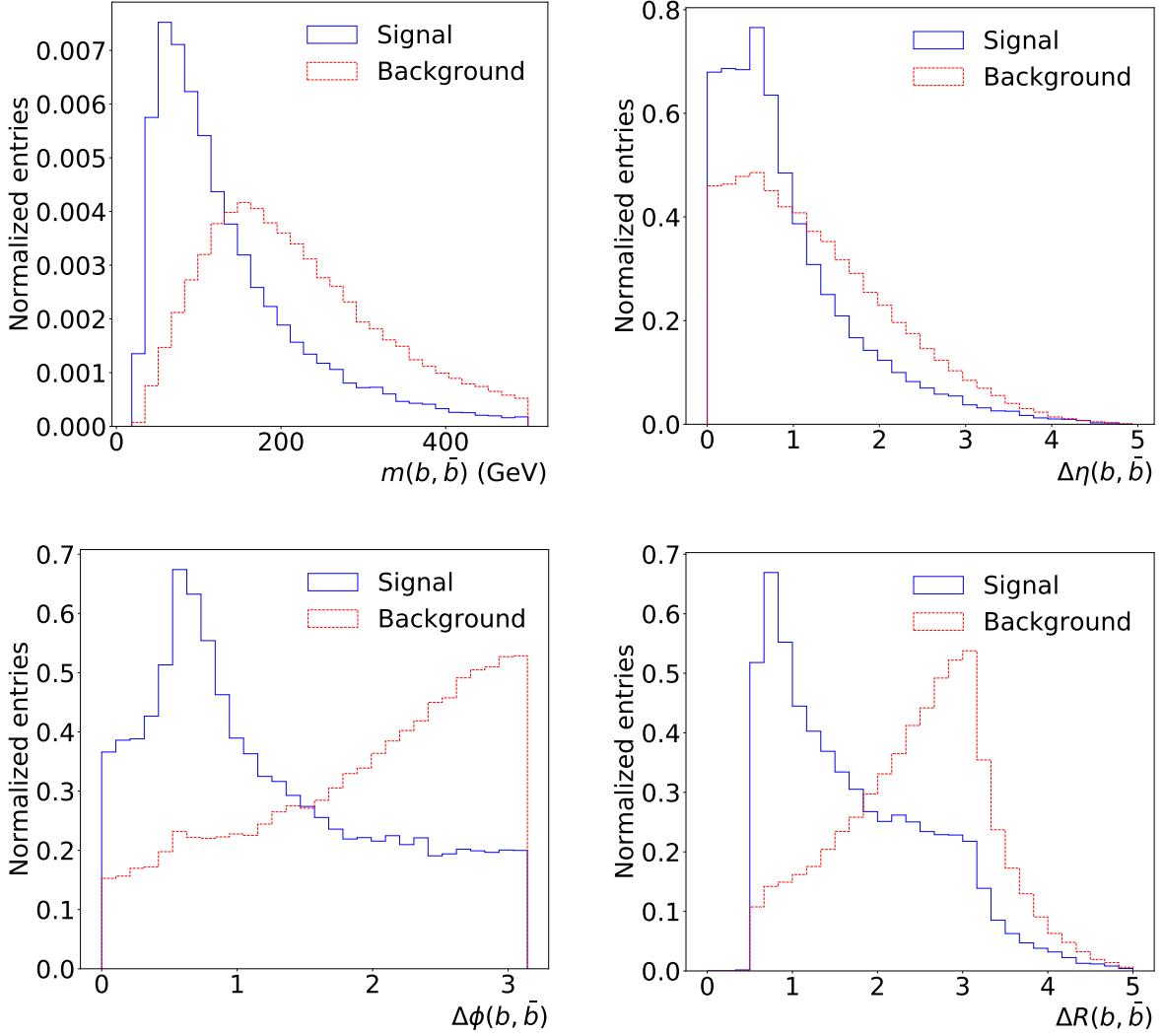


FIG. 4: Input variables of invariant mass,  $\Delta\eta$ ,  $\Delta\phi$  and  $\Delta R$  of two selected b jets (clockwise from upper left).

parameter space fixing the number of epochs as 100. The parameters are chosen in a way that the efficiency is the highest. This procedure is done for each event selection scenario. Figure 5 shows the matching efficiency in the 2D parameter space for number of nodes and layers after at least 4 jets and 4 b-tagged jets. We found that the efficiency is not sensitive in this parameter space. Therefore, as optimal point, 4 layers and 100 nodes per each layer are used throughout all the deep neural network models. The output scores from the training and test samples are shown together in Fig. 6. The distributions from both samples agree each other. This agreement shows that there is no overtraining in the model. For the 10k

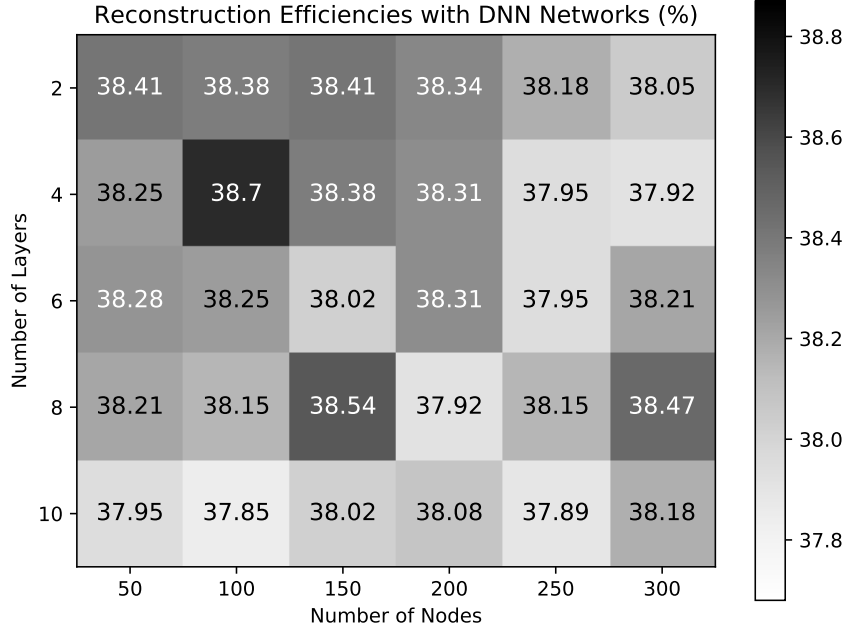


FIG. 5: Matching efficiency in 2D with different number of layers and nodes per each hidden layer ranges after the requirement of at least 4 jets and 4 b-tagged jets. The number of layers of 4 and the number of nodes of 100 are selected as the optimal numbers.

events, total training time costs almost 700 seconds using Nvidia Titan XP Graphic cards of 4 with 12 GB of RAM is used for this analysis.

Figure 7 shows the matching efficiencies in different requirements of number of jets and b-tagged jets together with the results from the minimum  $\Delta R$  analysis. The corresponding numbers are shown in Table IV. As shown in Fig. 7, overall the matching efficiency is getting larger when applying higher number of b-tagged jets. After the requirement of at least two b jets, around 23% matching efficiency is observed while it is 21% for the  $\Delta R$  method. Around 2% improvement is shown throughout the different number of jet requirements. For the requirement of at least 3 b jets, the matching efficiency of 33% is obtained, which is around 4% higher than the  $\Delta R$  method. With the requirement of at least 4 b jets, the matching efficiency goes up to 39%. This efficiency is 8% higher than the  $\Delta R$  method. In general, we could reach up to around 40% level matching efficiency using the deep neural network in the lepton+jets mode.

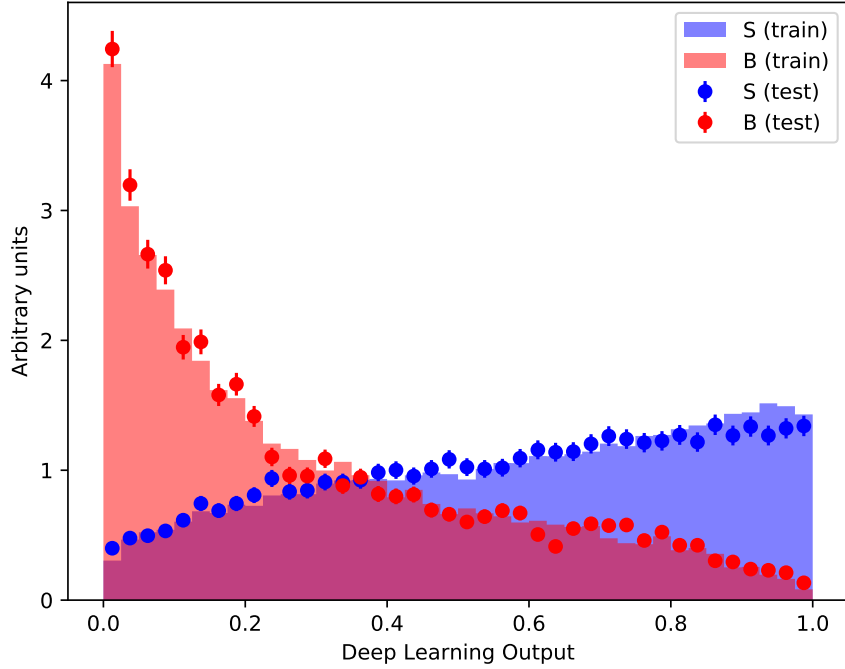


FIG. 6: Deep neural network output score for training and test samples. Test sample is indicated with dot. Two distributions for training and test datasets agree each other. This indicates that there is no overtraining. Only statistical uncertainty is given.

## VI. CONCLUSIONS

To measure the differential cross section as a function of properties of the additional b jets, the origin of the b jet needs to be identified. In this paper, we present the performance of identifying two additional b jets using simulated pp collision data at  $\sqrt{s} = 13$  TeV. Comparing with the minimum  $\Delta R$  analysis, the performance of deep neural network improves by 2-8% level depending on the number of b-tagged jet requirement. In particular, it is shown that requiring at least 4 b-tagged jets leads to better performance with the matching efficiency of around 40%. However, it would suffer from the lack of statistics with the current LHC data to apply this tight number of b-tagged jets. Using data from the Run-3 or the High Luminosity-LHC, it is conceivable to tighten the requirement of the number of b-tagged jets to improve the matching efficiency. In real analysis, more sophisticated high-level features are available. Optimizing those variables can lead us to improve the performance.

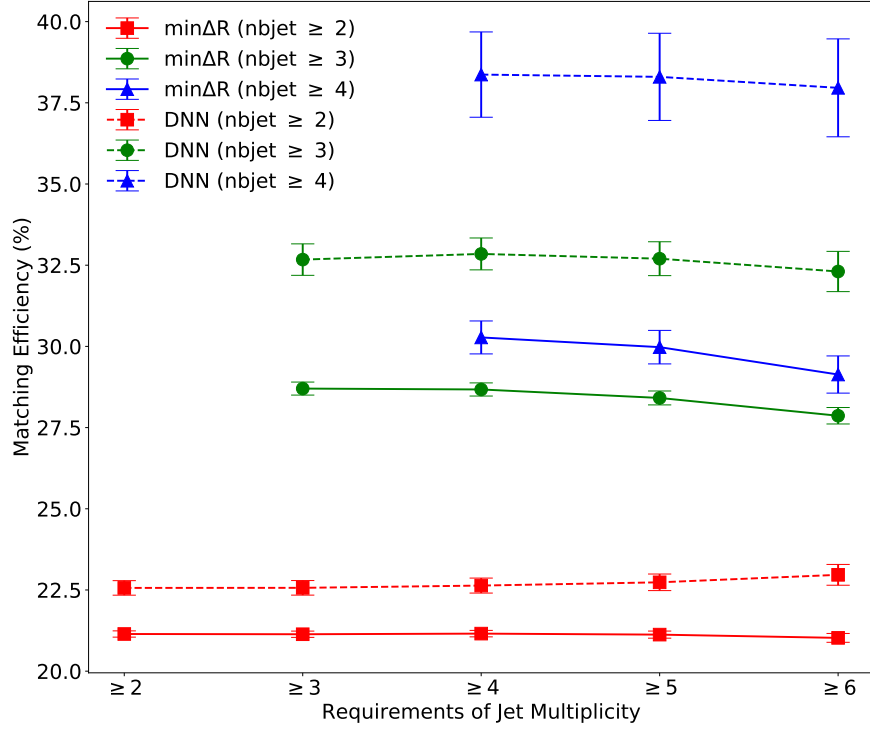


FIG. 7: Matching efficiency (dashed line) from the neural network comparing is shown together with the one from the minimum  $\Delta R$  analysis (solid line) as a function of number of jets. The results with different requirements of number of b-tagged jets are also shown with rectangle mark for 2 b-tagged jets, circle for 3 b-tagged jets and triangle for 4 b-tagged jets (color online).

### Acknowledgments

This work was supported by the research fund of Hanyang University (HY-2015). The work was also supported by Basic Science Research Program through the National Research Foundation of Korea (NRF) funded by the Ministry of Education, Grant No. NRF-2017R1A2B4002498.

- 
- [1] CMS collaboration, Phys. Rev. Lett. **120** (2018) 231801.
  - [2] ATLAS collaboration, Phys. Lett. B **784** (2018) 173.
  - [3] G. Bevilacqua and M. Worek, J. High Energy Phys. **07** 135 (2014).
  - [4] CMS collaboration, Phys. Lett. B **776** 355 (2018).

$N_j$	$N_b$	Matching Efficiency (%)	
		min. $\Delta R$	DNN
2	2	21.14	22.55
3		21.14	22.57
4		21.16	22.66
5		21.13	22.78
6		21.03	22.96
3	3	28.70	32.66
4		28.67	32.72
5		28.41	32.68
6		27.86	32.52
4	4	30.28	38.87
5		29.98	37.86
6		29.13	37.96

TABLE IV: Matching efficiencies for  $\Delta R$  analysis and DNN analysis for each event selection.

- [5] CMS collaboration, arXiv:1909.05306.
- [6] ATLAS collaboration, J. High Energy Phys. **04** (2019) 046.
- [7] CMS collaboration, Eur. Phys. J. C **76** (2016) 379.
- [8] J. Erdmann, T. Kallage, K. Kröninger, O. Nackenhorst, arXiv:1907.11181.
- [9] J. Alwall, R. Frederix, S. Frixione, V. Hirschi, F. Maltoni and et al., J. High Energy Phys. **07** (2014) 079.
- [10] Sjöstrand, Torbjörn et al., Comput. Phys. Commun. **191** (2015) 159-177.
- [11] P. Artoisenet, R. Frederix, O. Mattelaer and R. Rietkerk, J. High Energy Phys. **03** (2013) 015.
- [12] J. de Favereau, C. Delaere, P. Demin, A. Giammanco, V. Lemaître et al., J. High Energy Phys. **02** 057 (2014).
- [13] CMS collaboration, J. Instrum. **13** P05011 (2018).
- [14] S. Ioffe and C. Szegedy, arXiv:1502.03167.
- [15] N. Srivastava et al., JMLR **15** (2014) 19291958.